Nat Hazards (2008) 46:323–351
DOI 10.1007/s11069-007-9190-6

ORIGINAL PAPER

Implementation of reconstructed geomorphologic units in landslide susceptibility mapping: the Melen Gorge (NW Turkey)

T. Gorum · B. Gonencgil · C. Gokceoglu · H. A. Nefeslioglu

Received: 8 July 2007 / Accepted: 25 October 2007 / Published online: 7 March 2008
© Springer Science+Business Media B.V. 2008

Abstract In the international literature, although considerable amount of publications on the landslide susceptibility mapping exist, geomorphology as a conditioning factor is still used in limited number of studies. Considering this factor, the purpose of this article paper is to implement the geomorphologic parameters derived by reconstructed topography in landslide susceptibility mapping. According to the method employed in this study, terrain is generalized by the contours passed through the convex slopes of the valleys that were formed by fluvial erosion. Therefore, slope conditions before landsliding can be obtained. The reconstructed morphometric and geomorphologic units are taken into account as a conditioning parameter when assessing landslide susceptibility. Two different data, one of which is obtained from the reconstructed DEM, have been employed to produce two landslide susceptibility maps. The binary logistic regression is used to develop landslide susceptibility maps for the Melen Gorge in the Northwestern part of Turkey. Due to the high correct classification percentages and spatial effectiveness of the maps, the landslide susceptibility map comprised the reconstructed morphometric parameters exhibits a better performance than the other. Five different datasets are selected randomly to apply proper sampling strategy for training. As a consequence of the analyses, the most proper outcomes are obtained from the dataset of the reconstructed topographical parameters and geomorphologic units, and lithological variables that are implemented together. Correct classification percentage and root mean square error (RMSE) values of the validation

T. Gorum (✉)
Natural Sciences Research Center, Yildiz Technical University, Besiktas, 34349 Istanbul, Turkey
e-mail: tgorum@yildiz.edu.tr

B. Gonencgil
Department of Geography, Faculty of Letters, Istanbul University, Beyazit, Istanbul, Turkey

C. Gokceoglu
Department of Geological Engineering, Applied Geology Division, Hacettepe University, Beytepe, 06800 Ankara, Turkey

H. A. Nefeslioglu
Department of Geological Research, General Directorate of Mineral Research and Exploration, Balgat, 06520 Ankara, Turkey

dataset are calculated as 86.28% and 0.35, respectively. Prediction capacity of the different datasets reveal that the landslide susceptibility map obtained from the reconstructed parameters has a higher prediction capacity than the other. Moreover, the landslide susceptibility map obtained from the reconstructed parameters produces logical results.

Keywords Landslide susceptibility · Topographic reconstruction · Indirect mapping methods · GIS · Geomorphology · Melen Gorge (Turkey)

1 Introduction

Landslide is not only one of the important geomorphic hazards, but also a dynamic earth surface process contributing to the denudation and geomorphic evolution of the landforms. This dynamic process should be considered as an effect of natural landscape evolution. The interaction of this phenomenon with the anthropogenic activities causes important casualties and damages. Over the last decade, the developments in Geographic Information Systems (GIS) and landslide susceptibility analysis techniques have provided various facilities in applying landslide hazard mitigation programs. Given a set of geoenvironmental conditions, landslide susceptibility is the probability of spatial occurrence of known slope failures (Guzzetti et al. 2005). It is assumed that landslides will occur in the future because of the same conditions that produced them in the past (Guzzetti et al. 1999), susceptibility assessments can be used to predict the geographical location of future landslides (Chung and Fabbri 1999; Guzzetti et al. 2005). The methods of landslide susceptibility mapping are classified into two main groups as direct and indirect techniques. Direct methods, comprising heuristics approaches, can be assessed as direct geomorphologic mapping or qualitative map combination. In direct techniques, the geomorphologist or engineering geologist based on his/her experience and knowledge of the terrain conditions determines the degree of susceptibility directly (Van Westen et al. 2003). On the other hand, indirect methods such as statistical (bivariate or multivariate statistics), deterministic and knowledge-based artificial intelligence approaches are able to determine quantitatively the zonation of landslide susceptibility degree. Several applications on bivariate statistical methods (Clerici et al. 2002, 2006; Remondo et al. 2003; Suzen and Doyuran 2004a; Gokceoglu et al. 2005), multivariate statistical methods (Carrara 1983; Chung et al. 1995; Suzen and Doyuran 2004b; Can et al. 2005; Guzzetti et al. 2006; Lee and Pradhan 2007) and knowledge-based artificial intelligence methods (Lee et al. 2003a, b, 2004; Ercanoglu and Gokceoglu 2004; Yesilnacar and Topal 2005) and simple overlay method (Gokceoglu and Aksoy 1996) can be found in the literature.

One of the significant differences between these two techniques is the expert's opinion. While direct susceptibility map is produced depending on expert's opinion, the results of an indirect susceptibility map are interpreted by the expert. Parameters or factor maps that may be adopted in both techniques depend on one's experience and knowledge of the terrain conditions. However, the landslide susceptibility maps have some uncertainties resulting from the parameters employed and the techniques applied. In addition to the uncertainties about the parameter maps, an important uncertainty affecting the accuracy of the study is not mentioned frequently in landslide susceptibility assessment. Indirect landslide susceptibility map production requires a well-documented landslide inventory. Whichever method is used for indirect landslide susceptibility mapping, the conditioning parameters should be assessed with the landslide inventory altogether. The landslide inventories used in literature traditionally reflect the actual terrain conditions like failed

slopes. However, the question of what the terrain parameters, especially slope degree were at the failure time should be answered because one of the main targets of the landslide susceptibility maps is to determine the susceptibility degree of the slopes which has not failed yet. It is evident that this difference will affect the prediction capacity of the landslide susceptibility map. It is possible to prevent the failure of topographic features in advance by reconstruction method. The purpose of the present study is to produce the landslide susceptibility maps using actual and reconstructed topographic data, and to compare their results in order to answer the question mentioned previously is highly important for the future landslide susceptibility assessments.

Considering the purpose of the present study, the reconstruction method is employed, because the failed terrain conditions reflect the actual terrain conditions. However, throughout the methodology part of the study, the reconstruction approach is implemented to overcome the uncertainty mentioned previously. The geomorphology map of the study area is also used as a parameter map. This process is carried out by taking into account the previous morphometric conditions obtained from the reconstruction of the actual terrain conditions. In addition to the conventional parameters, geomorphology as a parameter map is also considered in landslide susceptibility maps that are produced by logistic regression. In literature, the present study which uses the geomorphologic units as a conditioning factor map in landslide susceptibility analyses is not unique. Van Westen et al. (2003) and Duman et al. (2006) also considered this parameter in their works; however, the actual field conditions were taken into account. In evaluating the importance of reconstructed geomorphology as a parameter in the production of landslide susceptibility maps, binary logistic regression technique is used.

2 General characteristics of the study area

The Melen Gorge and its close vicinity is one of the landslide-prone areas of the Western Black Sea region of Turkey (Fig. 1). The area covers approximately 108 km^2 surface area. The topographic elevation values of the area range from 0 to 720 m, with an average value of 185 m. Slope gradients computed from DEM vary between 0 and 50.2 degrees, while its average is 13.7 degrees. In the field, the typical Black Sea climate prevails, the region acquires precipitation almost in all seasons, maximum in fall, and its zones where marine effects cannot reach, transitions to continental climate are observed rarely. Meanwhile annual rainfall in the period of 1970 and 2006 is 847 mm. In the area, landslides are triggered mainly by intense and prolonged rainfall. As an example, the Dokuzdegirmen landslides which occurred on November 12th in 1995 after a prolonged rainfall period causes significant damages in the region. This intense rainfall episode continued during 4 days, and these two major landslides located very close to the town center of the Dokuzdegirmen district happened on the second day of this period (AIGM 1995). The lithological units of the study area are formed by sedimentary and volcanic rocks. The southern parts of the area are covered by volcanic units of Middle-Lower Eocene and sandstone-mudstone of Middle-Lower Eocene (Fig. 2). This sandstone-mudstone of Middle-Lower Eocene units covers 63% of the area's lithological units. The clayey limestones of Upper Cretaceous crop out in the central part of the area and form steep slopes. The steep slopes in the northern part of the study area are covered by Lower–Middle Eocene sandstone–mudstone (Tc) and Upper Cretaceous–Lower Eocene clayey limestones (Ktae) (Fig. 2). These units contain the majority of the landslides and comprise 95% of the actual landslides (Table 1). Pliocene conglomerate-sandstone crop out in the

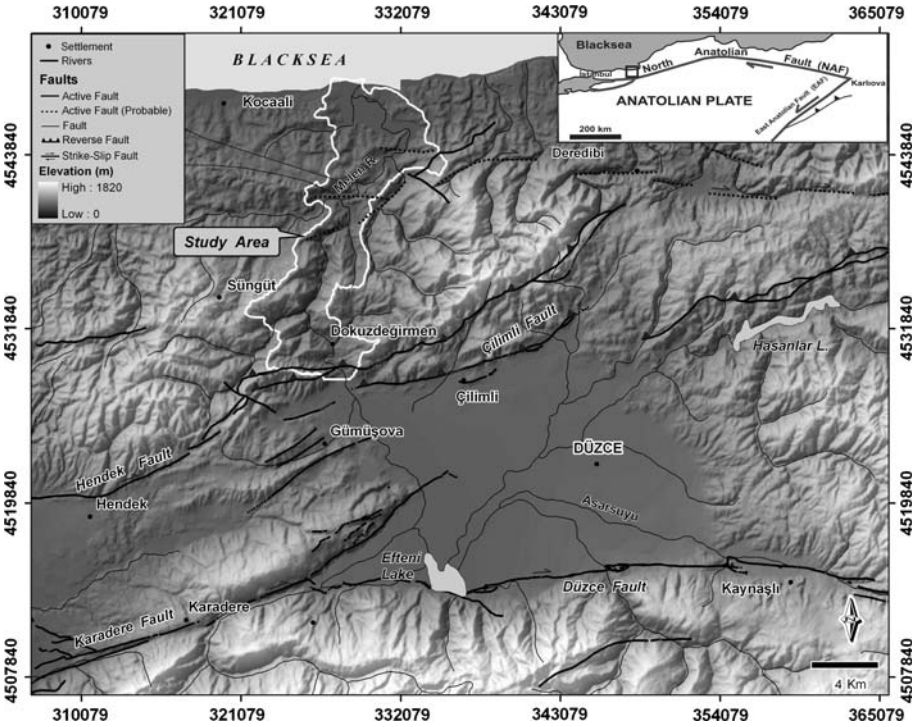


Fig. 1 Location map and major faults of the study area

northern parts of the area and recent alluvium in Quaternary age locates valley bottoms along the Melen River.

Physiographic features of the area are characterized by a steep and rough morphology formed by clayey limestone and sandstone-mudstone in the southern part. Deep valleys are present in this lithological composition in the central part. The northern parts of the area exhibit more gentle morphology than the southern part. This morphologic asymmetry is formed by the deformation zone of the North Anatolian fault zone (NAFZ). The NAFZ is 1600 km long right-lateral strike-slip and known as one of the most active fault zones in the world (Ketin 1948; Sengor 1979; Saroglu et al. 1987; Barka and Kadinsky-Cade 1988; Barka 1992; Gokasan et al. 2003). These faults controlling the general physiographic trend of the area, have been maintaining their activities effectively. An example is the Karadere–Duzce segment of the NAFZ (Fig. 1) that was ruptured during the Duzce earthquake with a magnitude of 7.2 (M_w) in 1999 (Emre et al. 1999) (Fig. 1). In this respect, besides the meteorological events, the other potential triggering factor for landsliding in the region can be considered as large earthquakes. One of well-known mass movement, located on the far south of the study area happened in 1999, during Duzce earthquake occurred on November 12th (Emre et al. 1999).

The geomorphology of the area is conditioned by the NAFZ and sea level changes during the Pliocene and Quaternary period. Morphology is dominated by denudational origin landforms (Fig. 3). These erosional landforms reflect a complex geomorphologic history of the area. In order to understand this complex history and landslide activities in the area, a generalized geomorphology map is prepared by employing the interpretation of

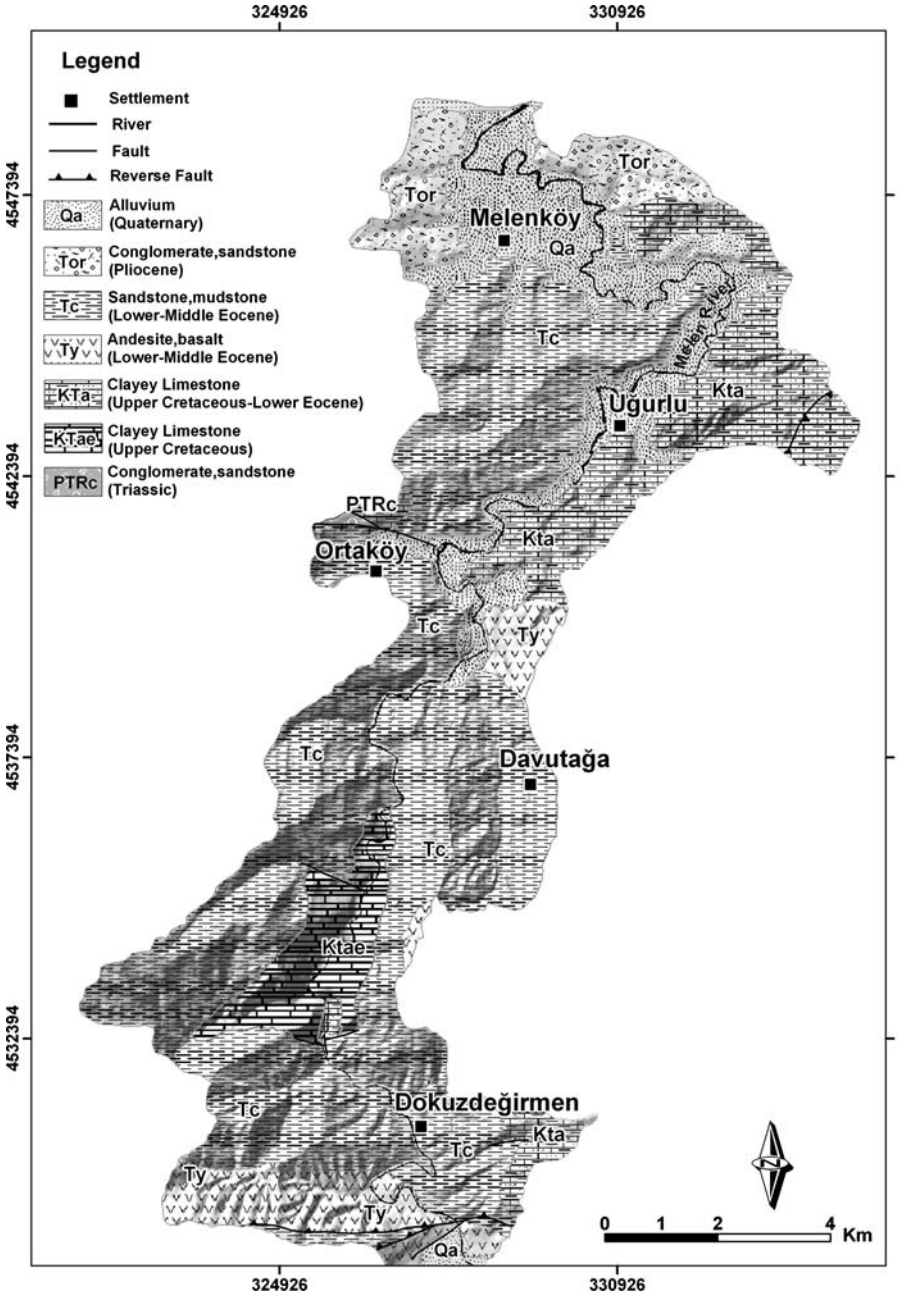


Fig. 2 Geology map of the study area (Ketin 1955; Pekcan 2000)

two sets of aerial photographs and extensive field works (Fig. 3). Landslides are the main agent of the geomorphologic complexities of the study area. A total of 82 landslides, varying in type and activity, are identified in the study area. Among these landslides, a total

Table 1 Landslide densities of the lithological units in the study area

Lithological units	Symbol	Grid cells with landslides		All grid cells		Landslide density (%)
		Frequency (no. of pix.)	%	Frequency (no. of pix.)	%	
Clayey limestone (Upper Cretaceous–Lower Eocene)	Kta	43	0.41	5,228	3.04	0.82
Clayey limestone (Upper Cretaceous)	Ktae	597	5.68	9,139	5.31	6.53
Conglomerate, sandstone (Triassic)	Ptrc	0	0.00	260	0.15	0.00
Alluvium (Quaternary)	Qa	1	0.01	25,993	15.10	0.00
Sandstone, mudstone (Lower–Middle Eocene)	Tc	9,491	90.37	109,686	63.73	8.65
Conglomerate, sandstone (Pliocene)	Tor	0	0.00	9,660	5.61	0.00
Andesite, basalt (Lower–Middle Eocene)	Ty	370	3.52	12,148	7.06	3.05

of 69 are classified as deep-seated circular and active according to the classifications proposed by Varnes (1978) and Cruden and Varnes (1996) (Fig. 4). The morphology of the 69 landslides (scarps, cracks, tilted and displaced blocks, hummocky topography) can be recognized clearly in the field.

3 Methodology

As mentioned previously, the main purpose of the present study is to investigate the effect of original topography (before slope failures) on the performance of landslide susceptibility maps. For this purpose, a reconstruction process should be applied. Reconstruction can be described as the obtaining of topographical conditions before slope failure by considering some morphological rules, such as slope orientations and contour trends. Although numerical models of landscape evolution are becoming commonplace, little agreement exists on what topographic measures should be used to compare model and real landscapes (Dietrich et al. 2003). As mentioned by Dietrich et al. (2003), a key issue is what features should be distinguished for the processes being responsible for landscape evolution. Obviously, morphometric parameters directly reflect these evolution mechanisms, using the measurable properties of landforms. During the reconstruction process of failed slopes, the morphometric parameters reflecting this evolution mechanism are used. However, the effects of erosion and active tectonic processes on the slope forming mechanism should not be disregarded because these processes might affect the reconstruction method employed in the present study. In the study area, the recent landslide activity is more intense than the erosion and active tectonic processes. For this reason, the reconstruction process employed in the present study is related directly with the landslides and therefore, erosion and active tectonic processes in short-period may be neglected. The primary effect of a slope failure on topographic environment is to change the morphology of the terrain where slope failure occurs. The secondary and the indirect effects are eminent because they influence the

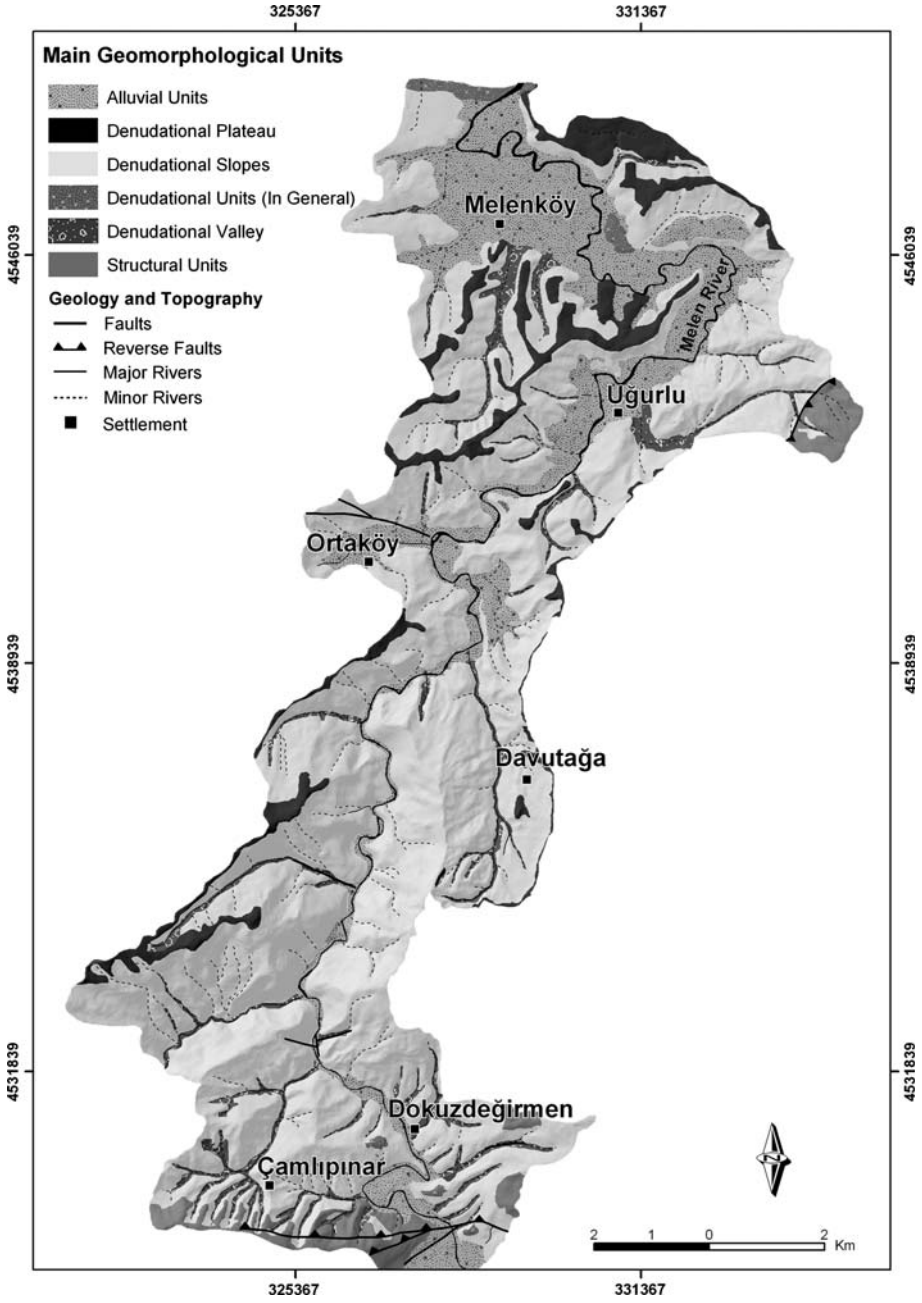


Fig. 3 Main geomorphologic units of the study area

primary and the secondary derivatives (such as altitude, slope gradient, aspect, slope curvature, and so forth) of the terrain. These topographic derivatives have been used for landslide susceptibility mapping as landslide conditioning parameters. It should be

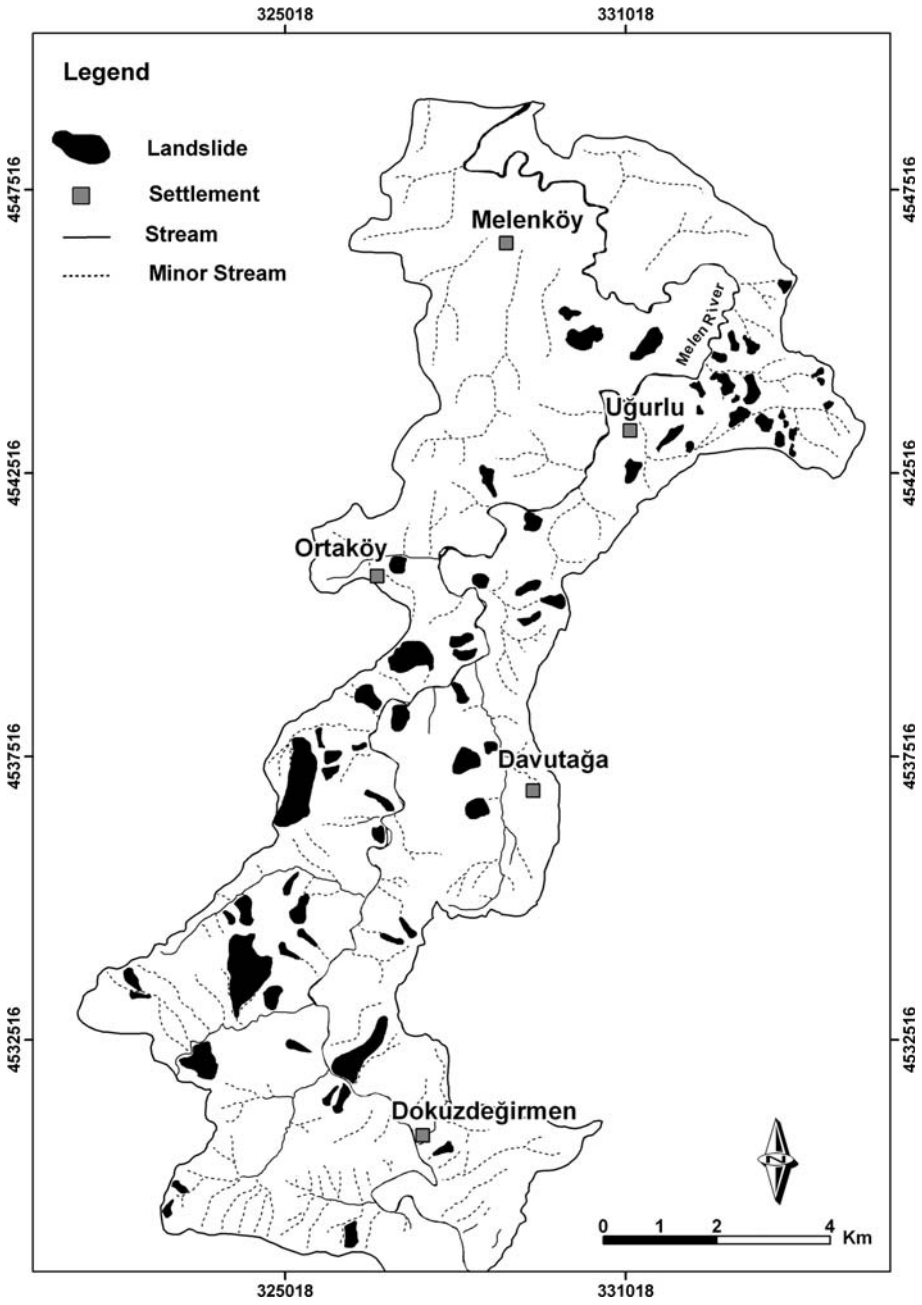


Fig. 4 Landslide inventory map of the study area

considered that utilization of geomorphologic parameters interpreted by using the reconstructed local terrain conditions into landslide susceptibility evaluations constitutes one of the main purposes of this study.

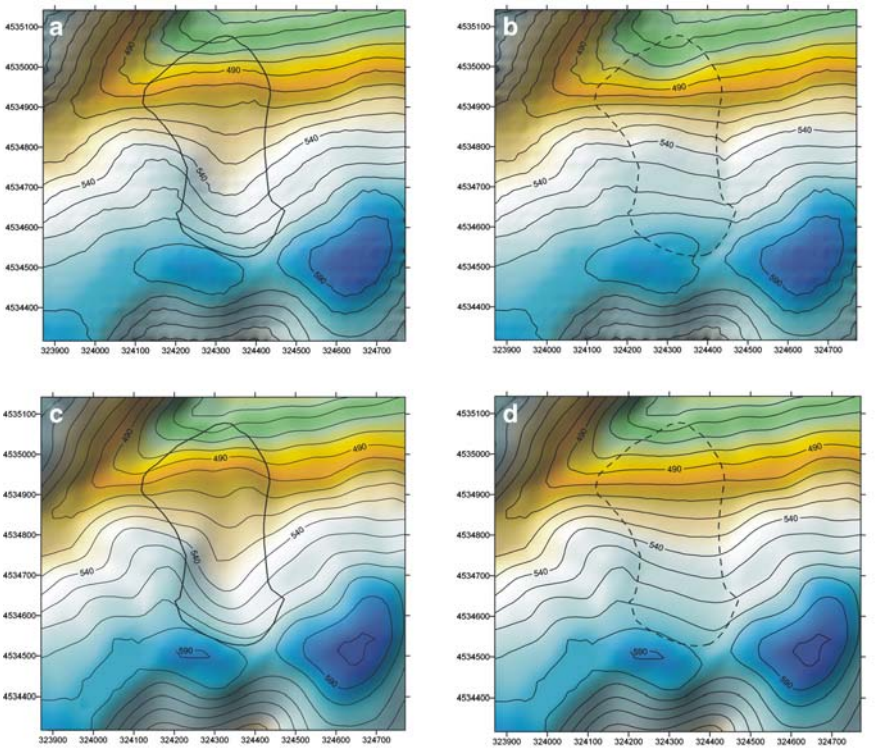
During the reconstruction process of the estimation of pre-failure topography by GIS methods, many interpolation methods such as Inverse Distance Weighted (IDW), Kriging, Natural Neighbor, Nearest Neighbor, Triangulation with Linear Interpolation are tested. IDW and Krigging interpolation methods show similar results. However, considering the slope orientations and the contour trends, more appropriate results are obtained from IDW (Fig. 5). IDW is based on one of the basic principles of geography and it declares that things which are close to each other are more alike (McCoy and Johnston 2001). In order to describe the location of an undefined terrain, one needs to look for the measured values within a specific neighborhood and estimate the value for this location. Hence, IDW estimates the final grid-cell value by averaging the values of the sample data points in the vicinity of this grid cell (Eq. 1).

$$z(x_0) = \frac{\sum_{i=1}^{n} \frac{1}{d_{ij}^p} z(x_i)}{\sum_{i=1}^{n} \frac{1}{d_{ij}^p}} \tag{1}$$

where "z" is the sample points, "d_{ij}" is the Euclidean distance between each data point and the point to interpolate, and "p" is the power value. This method assumes that the variable being mapped decreases in influence with distance from its sampled location (McCoy and Johnston 2001; Childs 2004). With the IDW, the significance of the interpolated values based on their distance from the output point can be controlled. The significances of the weights belonging to these data points are explained by the terms of power. If the rate of power is defined as high in a given area, the resulting surface will be more detailed. In this study, average and most commonly used power value "2" is taken into consideration. This weight value for the interpolated surface in the IDW method directly controls the search radius, limiting the number of input points that can be used for calculating each interpolated cell (McCoy and Johnston 2001).

The application of the proposed reconstruction methodology constitutes four main stages. First one is the re-grouping of landslides according to their slope orientations. Estimation of a topographical altitude using IDW algorithm is directly influenced by the acute angle between ridge orientation and movement direction. For this reason, considering the orientation of the main sector having the highest radius of the search ellipse, 8 different slope orientation groups (SOG) such as [0–45], [45–90] … [270–315], [315–360] were defined (Fig. 5). Pre-processing of digital elevation model (DEM) for the reconstruction is the second stage of the proposed method. For this purpose, at first, conversion of raster DEM to vector point data has to be accomplished. Then, the vector point data included in the landslide area is extracted from the original data. After this stage, some holes in the DEM are obtained. The essential of the proposed reconstruction method in this study is the estimation of new topographic altitude values representing pre-failure conditions in these holes by applying the interpolating technique IDW algorithm. Considered criteria for the reconstruction method in IDW algorithm are given in Fig. 5. Applying the IDW algorithm for each slope orientation group, the reconstructed topographic altitudes are obtained. As a consequence, the last stage is the merging the reconstructed values for each SOG with the rest of the original data, and here after the final reconstructed DEM is acquired.

In order to check the performance of the reconstruction methods proposed in this study, four different landslide masses having depth of failure surface predicted, salient depletion and zone of accumulation are considered (Fig. 6). For this purpose, the volumetric changes represented by unit area resolution between the topography reconstructed and the actual topography are calculated by using the reconstructed and actual digital elevation models. Theoretically, the total negative displacement on the depletion zone should be equal to the



Considered criteria for the reconstruction method (in IDW)

- Number of sectors to search : 32
- Maximum number of data to use from all sectors : 64
- Maximum number of data to use from each sectors : 6
- Minimum number of data in all sectors (node is blanked if fewer) : 8
- Blank node if more than this many sectors are empty : 16
- Search Elipse Radius : 1100 m
  Angle for orientation of ridges : 0-360°

Slope Orientation Group (SOG)

SOG-1; Slope Aspect (0-45°); θ = 45°
SOG-2; Slope Aspect (45-90°); θ = 0°
SOG-3; Slope Aspect (90-135°); θ = 45°
SOG-4; Slope Aspect (135-180°); θ = 90°
SOG-5; Slope Aspect (180-225°); θ = 45°
SOG-6; Slope Aspect (225-270°); θ = 0°
SOG-7; Slope Aspect (270-315°); θ =45°
SOG-8; Slope Aspect (315-360°); θ =90°

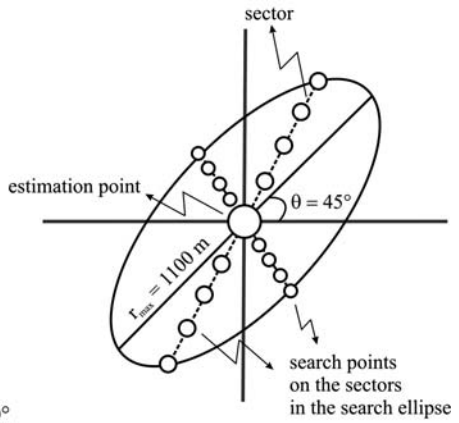


Fig. 5 Inverse distance weighted (IDW) vs. Kriging method and considered criteria for reconstruction method (in IDW); (**a**) Actual DEM interpolated in IDW, (**b**) Reconstructed DEM interpolated in IDW, (**c**) Actual DEM interpolated in Kriging method, (**d**) Reconstructed DEM interpolated in Kriging method

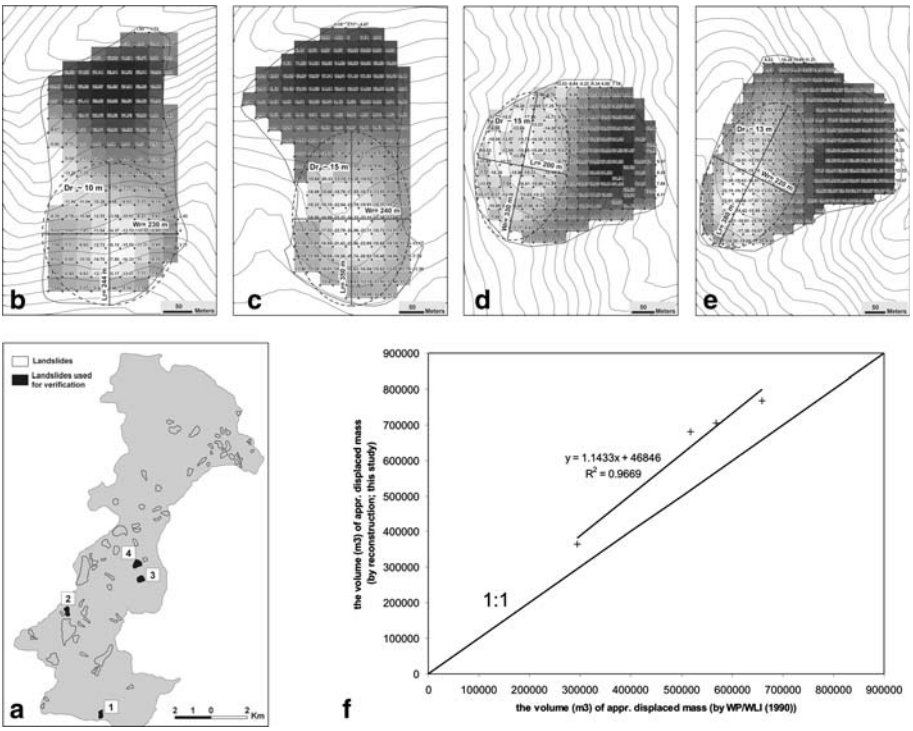


Fig. 6 Verification results for the reconstruction procedure applied in the study. (**a**) Location map of the landslides used for verification, (**b**, **c**, **d**, **e**) volumetric calculations, (**f**) crosschecks between the volumes calculated from both the equation proposed by Popescu (1990) and the reconstruction method suggested in this study

volume of the displaced material to be calculated by the equation (Eq. 2) proposed by the UNESCO Working Party on World Landslide Inventory (Popescu 1990). Considering this approach, a series of analyses are performed and the results are cross-correlated. According to the results of cross-correlation, the reconstruction method proposed in the present study produces acceptable results (Fig. 6).

$$V_{ls} = \frac{1}{6} \times \pi \times D_r \times W_r \times L_r \tag{2}$$

where V_{ls} is landslide volume; D_r is the depth of failure surface; W_r is the width of the depletion zone; L_r is the length of depletion zone.

4 Data production

In the study, landslides were collected and mapped by using the results of the interpretations of two sets of aerial photographs (1956 and 1976). They were also checked during the field studies. The mass movements identified by using two photo sets are merged into one vector file forming the landslide inventory map of the Melen Gorge. This inventory map represents a training source for the statistical analysis to understand the parameters controlling the mass movements (Fig. 4). Landslides cover an area of 6.56 km^2 in the study area, and this amount constitutes 6.07% of the study area. The minimum and the

maximum landslide areas are found as 0.01 and 0.7 km^2, respectively. In landslide susceptibility mapping techniques, uniformity of mass movement type is an important factor in the validation stage especially. In this respect, landslide susceptibility map is produced by considering only deep-seated circular types of landslides in the area.

The second dataset is formed by the geological map (Fig. 2). This dataset is derived from different scaled geological maps produced by the General Directorate of Mineral Research and Exploration (MTA) and other studies (Ketin 1955; Pekcan 2000). The geological dataset is also used to extract lithological characteristics of the area. In the area, the majority of the landslides (90.6%) occurred in the Eocene flyschoidal deposits (Tc). The main lithologies governing the landslides are the weak sandstone and mudstone layers. Highly fractured structural pattern of these formations cause such kind of peculiarities. For this reason, these units could be considered as one of the main conditioning factors of the landslides in the area. Considering the landslide distribution and particularly landslide densities (Table 1), the flyschoidal units (Tc) of Lower–Middle Eocene and the clayey limestone units of Upper Cretaceous (Ktae) are the most landslide-prone lithologies. In addition to these lithologies, volcanic rocks of Lower–Middle Eocene also contain some minor landslides but areal distribution of these landslides is rather low.

The third dataset is the digital topographical maps obtained from the General Command of Mapping of Turkey. Using this data, grid-based digital elevation model (DEM) having a ground resolution of 25 × 25 m of the region is constructed (Fig. 7a). The pixel size of 25 × 25 m provides optimum resolution conditions and data volume. In order to prepare the topographical parameter maps for the study area, the DEM is used. Besides these seven lithologic dichotomous (0, 1) variables of geology, seven topographical parameters such as altitude, slope, aspect, stream power index (SPI), topographic wetness index (TWI), plan curvature and profile curvature are taken into account as the possible conditioning factors

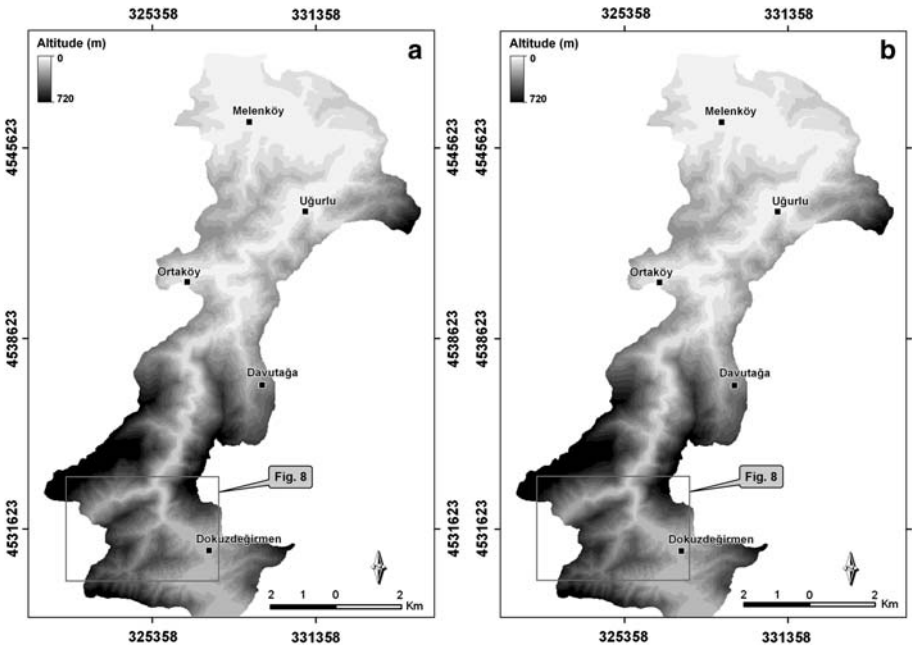


Fig. 7 Digital elevation model (DEM) of the study area; (**a**) Actual DEM, (**b**) Reconstructed DEM

for the landslides in the area. On the other hand, the actual DEM is reconstructed to obtain the reconstructed DEM representing the field conditions prior to landsliding (Fig. 7b). In this respect, the same derivation process is applied on the reconstructed DEM to obtain the topographical parameter maps. A sample area related to the actual and reconstructed topographical parameters is given in Fig. 8. Table 2 shows the descriptive statistics of the topographical parameters derived from these DEM's with respect to landslide inventory. For the spatial analyses, ArcView 3.2, ArcGIS 9 and Surfer 8 packages are used.

Although no agreement on topographical conditioning factors have to be used in landslide susceptibility analyses in literature, altitude, slope gradient, slope aspect, and slope curvatures are frequently used in landslide susceptibility studies. In addition, TWI and SPI, known as secondary topographic attributes in literature (Wilson and Gallant 2000), have been used in landslide susceptibility studies, recently (Gokceoglu et al. 2005; Yesilnacar and Topal 2005; Duman et al. 2006). SPI is used to describe potential channel erosion and landscape processes. Consequently, SPI is a measure of erosive power of water flow based on assumption that discharge (q) is proportional to specific catchment area (A_s) (Eq. 3) (Moore et al. 1991).

$$\mathrm{SPI} = A_s \tan \beta, \tag{3}$$

where A_s is the specific catchment area ($m^2\ m^{-1}$) while β is the slope gradient in degree. This index is one of the main factors controlling the erosion process and so is the main

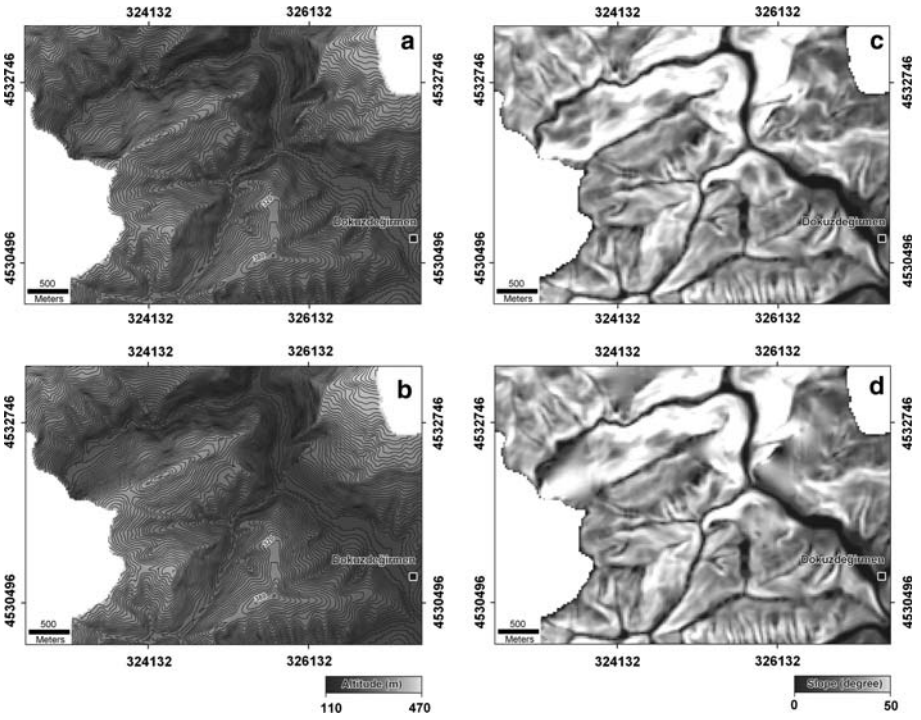


Fig. 8 An example for the topographical parameter maps produced from actual and reconstructed DEM (for location see Fig. 5); (**a**) Altitude and contour map produce from actual DEM, (**b**) Altitude and contour map produced from the reconstructed DEM (**c**) Slope gradient (degree) map produced from actual DEM, (**d**) Slope gradient (degree) map produced from the reconstructed DEM

Table 2 Descriptive statistics of topographical parameters with respect to landslide inventory

Data	Variable	Symbol	Min.	Max.	Mean	Mode	Median	Variance	Std. deviation	Skewness	Kurtosis
Actual topographic parameters, grid cells with landslide ($N = 10{,}502$)	Altitude (m)	Alt	10.00	693.2	247.28	231.82	90.00	22547.10	150.16	0.43	−0.75
	Slope gradient (degree)	Slp	0.00	43.87	15.57	14.64	10.41	40.29	6.35	0.75	0.65
	Slope aspect (degree)	Asp	−1.00	359.97	183.40	172.05	−1.00	13680.89	116.97	0.06	−1.38
	Stream power index	Spi	0.00	5.83	1.09	0.87	0.00	0.93	0.96	1.50	2.68
	Topographic wetness index	Twi	3.49	8.48	4.96	4.90	4.44	0.35	0.59	0.80	1.45
	Plan curvature	Plan	–2.27	2.11	−0.05	–0.04	0.00	0.09	0.30	−0.05	3.65
	Profile curvature	Prof	–1.97	1.75	0.03	0.02	0.00	0.08	0.28	0.15	3.95
Actual topographic parameters, grid cells without landslide ($N = 161{,}612$)	Altitude (m)	Alt	0.00	720	181.62	10.00	140.00	24373.70	156.12	0.92	0.07
	Slope gradient (degree)	Slp	0.00	50.08	13.14	0.00	12.59	86.28	9.29	0.45	−0.33
	Slope aspect (degree)	Asp	−1.00	360	163.96	−1.00	152.05	13437.12	115.92	0.11	−1.32
	Stream power index	Spi	0.00	9.78	0.78	0.00	0.45	1.12	1.06	2.84	11.61
	Topographic wetness index	Twi	3.26	18.98	5.68	4.62	5.02	4.12	2.03	2.65	8.89
	Plan curvature	Plan	−2.95	3.23	0.01	0.00	0.00	0.11	0.33	−0.33	5.84
	Profile curvature	Prof	−4.25	3.47	0.01	0.00	0.00	0.14	0.37	−0.06	5.90
Reconstructed topographic parameters, grid cells with landslide ($N = 10{,}502$)	Altitude (m)	Alt	12.27	697.36	255.24	90.00	224.35	24412.49	156.24	0.45	−0.82
	Slope gradient (degree)	Slp	0.00	39.96	15.14	0.00	14.66	41.16	6.42	0.45	0.29
	Slope aspect (degree)	Asp	−1.00	359.97	185.08	−1.00	165.46	14246.61	119.36	0.07	−1.35
	Stream power index	Spi	0.00	4.9	1.17	0.00	1.05	0.76	0.87	0.91	0.78
	Topographic wetness index	Twi	3.70	10.14	5.03	4.94	4.96	0.41	0.64	1.44	5.23
	Plan curvature	Plan	−2.67	2.1	−0.01	0.00	−0.01	0.05	0.21	0.08	13.63
	Profile curvature	Prof	−1.98	1.84	0.00	0.00	−0.01	0.04	0.21	0.36	10.75

Table 2 continued

Data	Variable	Symbol	Min.	Max.	Mean	Mode	Median	Variance	Std. deviation	Skewness	Kurtosis
Reconstructed topographic parameters, grid cells without landslide ($N = 161{,}612$)	Altitude (m)	Alt	0.00	720	181.68	10.00	140.00	24407.52	156.23	0.92	0.07
	Slope gradient (degree)	Slp	0.00	50.08	13.01	0.00	12.41	85.39	9.24	0.47	−0.30
	Slope aspect (degree)	Asp	−1.00	360	163.79	−1.00	152.28	13469.39	116.06	0.11	−1.31
	Stream power index	Spi	0.00	9.78	0.79	0.00	0.46	1.14	1.07	2.78	11.09
	Topographic wetness index	Twi	3.26	18.98	5.70	4.67	5.04	4.10	2.03	2.63	8.77
	Plan curvature	Plan	−2.95	5.84	0.01	0.00	0.00	0.11	0.33	−0.22	6.90
	Profile curvature	Prof	−4.25	3.47	0.01	0.00	0.00	0.14	0.37	−0.11	6.20

conditioning factor of landslide occurrence (Duman et al. 2006). The other index, TWI, has been used extensively to describe the effect of topography on the location and size of saturated source areas of runoff generation (Moore et al. 1991), and it is a useful parameter as a conditioning factor in landslide susceptibility studies (Eq. 4).

$$\mathrm{TWI} = \ln\left(A_s / \tan\,\beta\right) \tag{4}$$

where A_s is the specific catchment area ($m^2\ m^{-1}$), β is the slope gradient in degree.

In addition to these parameters, a geomorphologic map is prepared based on the interpretation of these three datasets (aerial photographs, geology and topographic variables) and extensive field studies (Fig. 9a). In the study area, polygon-based classification system for the geomorphologic mapping is preferred. The reason behind the preference is a conventional geomorphologic mapping system including different symbols, and lines and hatchings. When producing the geomorphologic map of the area, relations among geomorphologic origin, morphometric classifications (internal relief, micro relief, and slope classes, etc), physiographic classifications (land systems to land elements) and lithological variables are considered. Geomorphologic units consist of 469 different polygons and 28 legend classes. The legend represents information on the genesis, physiographic properties and morphometric information of the map (Fig. 9a). On the other hand, this geomorphologic unit map is reconstructed to obtain geomorphology parameter map. Following this process, a new map (the reconstructed geomorphologic unit map) is obtained (Fig. 9b). The new map consists of 353 different polygons and 26 legend classes. Following this stage, the polygon-based vector dataset is converted to grid data structure with ground resolution of 25 $\times$ 25 m to be used in the analyses as a parameter map. Areal distributions of different geomorphologic units with respect to landslide inventory are given in Table 3. Considering the landslide distribution and especially landslide densities (Table 3), slopes such as; moderately to severely dissected slopes (Msd), slightly to moderately dissected slopes (Smd), steep slopes (Ss) and slightly dissected slopes (in mainly gully erosion) (Sdg) are obtained as the most landslide-prone geomorphologic units in the area.

5 Susceptibility analyses

For the study area, a landslide susceptibility map is prepared using logistic regression analysis using 40 geoenvironmental variables such as altitude, slope gradient, slope aspect, profile and plan slope curvatures, SPI, TWI, lithology and geomorphology. In order to determine degree of landslide susceptibility, grid cells as terrain mapping unit are used considering extend of the study area and landslide distribution in the region. The study area is comprised of total of 172,114 grid cells, 10,502 of which contain landslides. Landslide susceptibility evaluation involves a high level of uncertainty due to data limitation and model shortcomings (Zezere 2002). In this respect, the landslide researchers have considered different techniques to prepare landslide susceptibility maps. One of the multivariate statistical techniques is logistic regression. In literature, the logistic regression technique is widely used in producing landslide susceptibility maps (e.g., Atkinson and Massari 1998; Gorsevski et al. 2000; Lee and Min 2001; Ohlmacher and Davis 2003; Lee 2004, 2005; Ayalew and Yamagishi 2005; Can et al. 2005; Duman et al. 2006; Nefeslioglu et al. 2007). The fundamental principle of logistic regression is based on the analysis of a problem, in which a result measured with dichotomous variables (such as zero and one or true and false) is determined from one or more independent factors (Menard 1995). In the case of landslide susceptibility mapping, the aim of logistic regression would be to find the

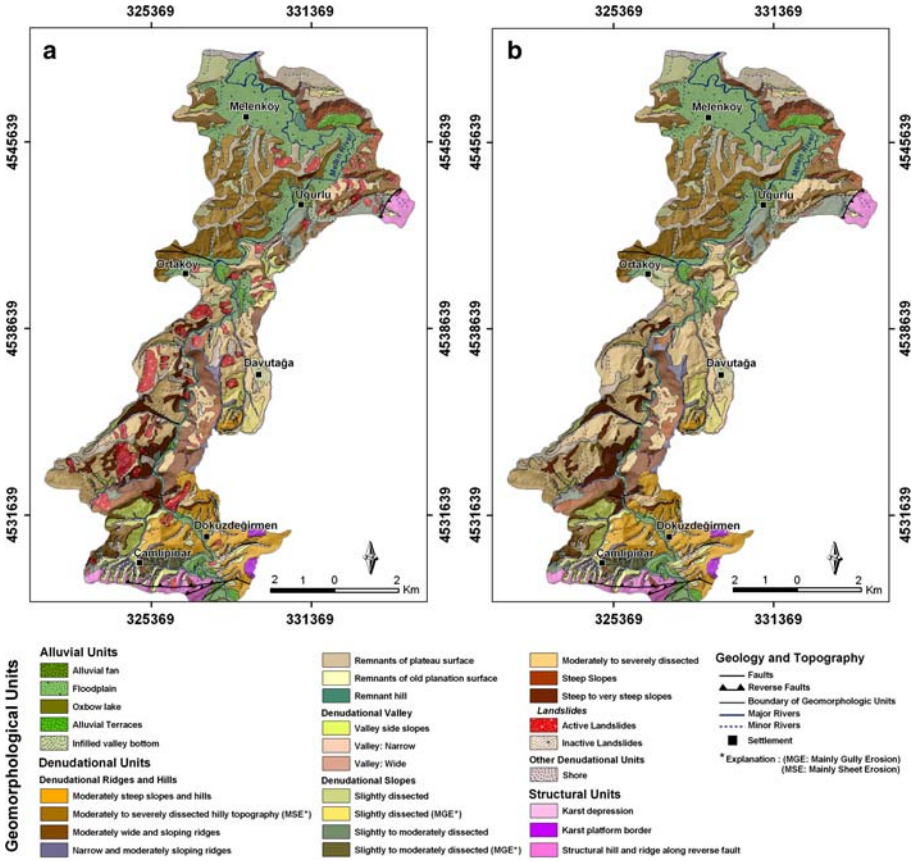


Fig. 9 Geomorphologic units of the study area; (**a**) Actual geomorphologic unit map, (**b**) Reconstructed geomorphologic unit map

best fitting model in order to describe the relationship between the presence or absence of landslides (dependent variable) and a set of independent parameters such as altitude, slope (degree), and SPI. In general, logistic regression involves fitting the dependent variable using an equation in the following form:

$$Y = \text{logit}(P) = \ln\left(p/(1-p)\right) = c_0 + c_1x_1 + \cdots + c_nx_n \tag{5}$$

where p is the probability that the dependent variable (Y) is 1, $p/(1-p)$ is the so-called odds or likelihood ratio, C_0 is the intercept, and C_1, C_2,...,C_n are coefficients that measure the contribution of independent factors (X_1, X_2,...,X_n) to the variations in Y. In this study, the dependent variable is defined as the presence or absence of landslide deposits, while the independent variables are those thought to affect landslide susceptibility. An overall of 7 topographical parameters (continuous variables) and 7 lithological and 26 geomorphologic units in binary format (dummy variables), a total of 40 independent variables are included in the logistic regression analyses. The dependent variable used in the analyses is also expressed in binary format with respect to presence (1) and absence (0) of landslide occurrences. One of the main requests of the multivariable statistical applications is the equal sampling strategy for the training dataset (Ayalew and Yamagishi 2005; Can et al.

Table 3 Landslide densities of the geomorphological units in the study area

Geomorphological units	Symbol	Grid cells with landslides		All grid cells		Landslide density (%)
		Frequency (no. of pix.)	%	Frequency (no. of pix.)	%	
Alluvial fan	Af	0	0.00	929	0.54	0.00
Beach	Bch	0	0.00	786	0.46	0.00
Floodplain	Fp	2	0.02	27,408	15.92	0.01
Infilled valley bottom	Ivb	0	0.00	2,018	1.17	0.00
Karst depression	Kd	0	0.00	32	0.02	0.00
Karst platform border	Kpb	0	0.00	743	0.43	0.00
Moderately to severely dissected	Msd	5,793	55.16	33,378	19.39	17.36
Moderately to severely dissected hilly topography	Msdh	716	6.82	12,024	6.99	5.95
Moderately to severely dissected hilly topography (MSE)	Msdhs	463	4.41	16,234	9.43	2.85
Moderately wide and sloping ridges	Mwsr	509	4.85	8,549	4.97	5.95
Narrow and moderately sloping ridges	Nms	119	1.13	2,218	1.29	5.37
Oxbow lake	Olk	0	0.00	108	0.06	0.00
Remnant hill	Rh	0	0.00	330	0.19	0.00
Remnants of old planation surface	Rops	0	0.00	263	0.15	0.00
Remnants of plateau surface	Rps	751	7.15	11,889	6.91	6.32
Slightly dissected	Sd	131	1.25	4,324	2.51	3.03
Slightly dissected (MGE)	Sdg	196	1.87	2,967	1.72	6.61
Slightly to moderately dissected	Smd	661	6.29	4,163	2.42	15.88
Slightly to moderately dissected (MGE)	Smdg	0	0.00	1,310	0.76	0.00
Steep slopes	Ss	524	4.99	6,955	4.04	7.53
Steep to very steep slopes	Svss	368	3.50	12,717	7.39	2.89
Structural hill and ridge along reverse fault	Shrarf	227	2.16	4,894	2.84	4.64
Alluvial terraces	Trc	0	0.00	2,682	1.56	0.00
Valley side slopes	Vss	37	0.35	8,922	5.18	0.41
Valley: narrow	Vn	0	0.00	4,519	2.63	0.00
Valley: wide	Vw	5	0.05	1,752	1.02	0.29

2005). This means that the ratio of presence (1) to absence (0) should be equal to 1 in the training dataset. For this purpose, a random data selection is applied to the absence (0) data. As the validation dataset, 20% of the presence (1) data (2100 grid cells are selected randomly) is excluded from the training dataset. While whole data matrix is comprised of 172,114 cases, the training dataset contains 16,804 cases. By using the training dataset, backward step-wise logistic regression analysis is carried out. It is performed continuously within a 95% confidence interval. Classification cut-off value and maximum iteration are selected as 0.5 and 12 respectively. In order to obtain the most appropriate results with the actual and the reconstructed datasets, a series of sensitivity analyses are performed as well. For this purpose, five different datasets, as given below, are constructed considering conditioning factors used and sampling strategies applied for training datasets in the study.

Dataset 1—only topographic parameters are produced from the actual DEM, 80% of presence (1) data is extracted from the landslide inventory randomly for the training dataset.

Dataset 2—only topographic parameters are produced from the reconstructed DEM, 80% presence (1) data is obtained from the landslide inventory randomly for the training dataset.

Dataset 3—topographic parameters are produced from the reconstructed DEM and lithological factors, 80% presence (1) data is obtained from the landslide inventory randomly for the training dataset.

Dataset 4—topographic parameters are produced from the reconstructed DEM and geomorphologic units, 80% presence (1) data is obtained from the landslide inventory randomly for the training dataset.

Dataset 5—topographic parameters are produced from the reconstructed DEM, lithological factors and geomorphologic units, 80% presence (1) data is obtained from the landslide inventory randomly for the training dataset.

Using these different datasets in logistic regression analyses, five different susceptibility maps are produced and four comparisons are made (Fig. 10). As a result of the backward step-wise logistic regression analysis, correct classification percentages for the prediction of presence (1) data in the training datasets are 63.5% for the Dataset 1, 67.4% for the Dataset 2, 86.8% for the Dataset 3, 78.9% for the Dataset 4 and 85.8% for the Dataset 5. As a consequence of the comparison between the actual and the reconstructed topographical parameters, considering the high correct classification percentages and spatial effectiveness of the reconstructed topographical parameters in the dataset 2, it can be evidently realized that the reconstruction process is essential. Topographical parameters such as altitude, slope gradient, slope aspect, TWI and SPI were found as significant (for the level of 0.05) statistically (Table 4). On the other hand, only slope and SPI are found as meaningful according to test statistics in all datasets. Considering the Wald test statistical values, the flyschoidal units of Lower–Middle Eocene (Tc) and the clayey limestone (Ktae) units of Upper Cretaceous are the main landslide conditioning factors among the lithological units as forecasted. Landslide densities of these lithologies are considerably high in the area (see Table 1; Tables 5 and 6). As the Wald test statistical values and the significance of β coefficients increase, the positive β coefficient values in test statistics of the variables in the equation also increase the possibility of landslide. Geomorphologic units are used in the datasets 4 and 5. Among geomorphologic units, moderately to severely dissected slopes (Msd), slightly to moderately dissected slopes (Smd), moderately to severely dissect hilly topography (Msdh) and structural hill and ridge along reverse fault (Shrarf) are the main landslide conditioning factors. As shown in Table 6, floodplain (Fp) and narrow valley (Vn) decrease the landslide possibility due to their morphological characteristics.

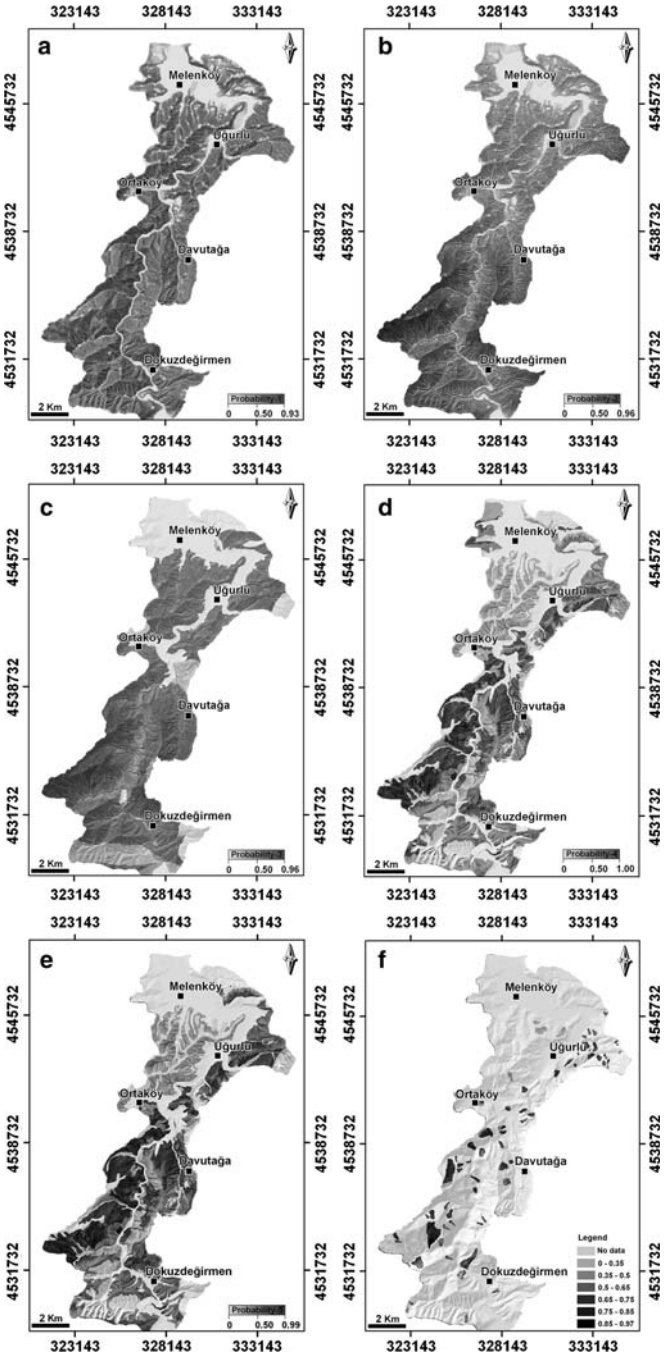


Fig. 10 Landslide susceptibility maps; (**a**) for the dataset 1, (**b**) for the dataset 2, (**c**) for the dataset 3, (**d**) for the dataset 4, (**e**) for the dataset 5, and (**f**) distributions of the susceptibility values—obtained from the dataset 5—on the observed landslides

Table 4 Beta (β) coefficients and test statistics of the variables in the equation with respect to datasets 1 and 2

Data	Variable	Symbol	β	Std. error	Wald	Degrees of freedom	Significance	Exp (β)
Dataset 1	Altitude (m)	Alt	−0.001	0.000	24.322	1.000	0.000	0.999
	Slope gradient (degree)	Slp	−0.074	0.005	209.400	1.000	0.000	0.929
	Slope aspect (degree)	Asp	0.000	0.000	8.322	1.000	0.004	1.000
	Stream power index	Spi	0.352	0.026	185.364	1.000	0.000	1.422
	Topographic wetness index	Twi	−1.236	0.053	541.715	1.000	0.000	0.290
	Plan curvature	Plan	−0.481	0.071	45.632	1.000	0.000	0.618
	Profile curvature	Prof	0.151	0.060	6.275	1.000	0.012	1.164
	Constant		7.271	0.332	479.470	1.000	0.000	1438.008
Dataset 2	Altitude (m)	Alt	0.002	0.000	373.501	1.000	0.000	1.002
	Slope gradient (degree)	Slp	−0.061	0.004	273.990	1.000	0.000	0.940
	Slope aspect (degree)	Asp	0.001	0.000	17.007	1.000	0.000	1.001
	Stream power index	Spi	0.447	0.020	510.194	1.000	0.000	1.564
	Topographic wetness index	Twi	−0.670	0.032	448.248	1.000	0.000	0.512
	Plan curvature	Plan	−0.075	0.065	1.311	1.000	0.252	0.928
	Profile curvature	Prof	0.025	0.060	0.176	1.000	0.675	1.025
	Constant		3.363	0.208	261.146	1.000	0.000	28.873

Table 5 Beta (β) coefficients and test statistics of the variables in the equation with respect to datasets 3 and 4

Data	Variable	Symbol	β	Std. error	Wald	Degrees of freedom	Significance	Exp (β)
Dataset 3	Altitude (m)	Alt	0.002	0.000	213.883	1.000	0.000	1.002
	Slope gradient (degree)	Slp	−0.048	0.004	134.465	1.000	0.000	0.954
	Slope aspect (degree)	Asp	0.001	0.000	26.500	1.000	0.000	1.001
	Stream power index	Spi	0.372	0.021	328.890	1.000	0.000	1.451
	Topographic wetness index	Twi	−0.335	0.036	85.951	1.000	0.000	0.715
	Clayey Limestone (Upper Cretaceous−Lower Eocene)	Kta	−1.456	0.189	59.539	1.000	0.000	0.233
	Clayey Limestone (Upper Cretaceous)	Ktae	1.082	0.100	116.232	1.000	0.000	2.952
	Conglomerate,sandstone (Triassic)	Ptrc	−12.237	232.440	0.003	1.000	0.958	0.000
	Alluvium (Quaternary)	Qa	−5.430	1.005	29.180	1.000	0.000	0.004
	Sandstone, mudstone (Lower−Middle Eocene)	Tc	1.251	0.074	284.887	1.000	0.000	3.494
	Conglomerate, sandstone (Pliocene)	Tor	−11.827	32.006	0.137	1.000	0.712	0.000
	Constant		0.621	0.245	6.418	1.000	0.011	1.861
Dataset 4	Altitude (m)	Alt	0.001	0.000	20.003	1.000	0.000	1.001
	Slope gradient (degree)	Slp	−0.017	0.003	23.562	1.000	0.000	0.984
	Stream power index	Spi	0.579	0.026	482.756	1.000	0.000	1.784
	Profile curvature	Prof	0.141	0.065	4.684	1.000	0.030	1.151
	Floodplain	Fp	−2.664	1.106	5.800	1.000	0.016	0.070
	Moderately to severely dissected	Msd	6.585	0.466	199.502	1.000	0.000	724.168
	Moderately to severely dissected hilly topography	Msdh	5.539	0.470	139.071	1.000	0.000	254.380
	Moderately to severely dissected hilly topography (MSE)	Msdhs	4.760	0.469	102.913	1.000	0.000	116.700
	Moderately wide and sloping ridges	Mwsr	5.653	0.472	143.545	1.000	0.000	285.051
	Narrow and moderately sloping ridges	Nms	5.621	0.489	132.202	1.000	0.000	276.100
	Remnants of plateau surface	Rps	5.771	0.470	150.851	1.000	0.000	320.860
	Slightly dissected	Sd	4.972	0.480	107.197	1.000	0.000	144.325
	Slightly dissected (MGE)	Sdg	5.355	0.479	124.905	1.000	0.000	211.570
	Structural hill and ridge along reverse fault	Shrarf	5.137	0.477	116.021	1.000	0.000	170.288

Table 5 continued

Data	Variable	Symbol	β	Std. error	Wald	Degrees of freedom	Significance	Exp (β)
	Slightly to moderately dissected	Smd	6.556	0.474	191.654	1.000	0.000	703.534
	Steep slopes	Ss	5.645	0.473	142.727	1.000	0.000	282.954
	Steep to very steep slopes	Svss	4.574	0.474	93.258	1.000	0.000	96.951
	Valley: narrow	Vn	−9.064	45.455	0.040	1.000	0.842	0.000
	Valley side slopes	Vss	2.663	0.502	28.118	1.000	0.000	14.345
	Constant		−5.913	0.468	159.955	1.000	0.000	0.003

Table 6 Beta (β) coefficients and test statistics of the variables in the equation with respect to dataset 5

Data	Variable	Symbol	β	Std. error	Wald	Degrees of freedom	Significance	Exp (β)
Dataset 5	Slope gradient (degree)	Slp	−0.025	0.006	21.014	1.000	0.000	0.975
	Stream power index	Spi	0.534	0.028	364.391	1.000	0.000	1.706
	Topographic wetness index	Twi	0.119	0.050	5.665	1.000	0.017	1.127
	Profile curvature	Prof	0.155	0.067	5.261	1.000	0.022	1.167
	Clayey Limestone (Upper Cretaceous−Lower Eocene)	Kta	−1.502	0.205	53.465	1.000	0.000	0.223
	Clayey Limestone (Upper Cretaceous)	Ktae	1.152	0.141	67.010	1.000	0.000	3.164
	Conglomerate,sandstone (Triassic)	Ptrc	−11.523	232.212	0.002	1.000	0.960	0.000
	Alluvium (Quaternary)	Qa	−4.520	1.017	19.758	1.000	0.000	0.011
	Sandstone, mudstone (Lower−Middle Eocene)	Tc	0.849	0.103	67.420	1.000	0.000	2.337
	Conglomerate, sandstone (Pliocene)	Tor	−12.346	29.440	0.176	1.000	0.675	0.000
	Floodplain	Fp	−2.701	1.119	5.831	1.000	0.016	0.067
	Moderately to severely dissected	Msd	6.367	0.472	181.584	1.000	0.000	582.247
	Moderately to severely dissected hilly topography	Msdh	5.407	0.476	128.828	1.000	0.000	222.910
	Moderately to severely dissected hilly topography (MSE)	Msdhs	4.381	0.476	84.844	1.000	0.000	79.939
	Moderately wide and sloping ridges	Mwsr	5.553	0.479	134.244	1.000	0.000	258.119
	Narrow and moderately sloping ridges	Nms	5.518	0.496	123.765	1.000	0.000	249.169
	Remnants of plateau surface	Rps	5.535	0.477	134.902	1.000	0.000	253.386
	Slightly dissected	Sd	4.890	0.489	99.936	1.000	0.000	132.956
	Slightly dissected (MGE)	Sdg	5.174	0.485	113.757	1.000	0.000	176.649
	Structural hill and ridge along reverse fault	Shrarf	6.099	0.490	154.927	1.000	0.000	445.339
	Slightly to moderately dissected	Smd	6.330	0.480	173.939	1.000	0.000	561.413
	Steep slopes	Ss	5.529	0.479	133.011	1.000	0.000	251.887
	Steep to very steep slopes	Svss	4.461	0.481	85.955	1.000	0.000	86.560
	Valley: narrow	Vn	−9.217	44.098	0.044	1.000	0.834	0.000
	Valley side slopes	Vss	2.693	0.508	28.084	1.000	0.000	14.775
	Constant		−6.722	0.583	132.835	1.000	0.000	0.001

When comparing different datasets according to their correct classification percentages and spatial effectiveness of maps, it is evident that the prediction performances are improved noticeably by using the reconstructed topographical parameters, lithological variables and geomorphologic units altogether. Applying the β coefficients obtained from different datasets in logistic regression equations, five different susceptibility maps are produced (Fig. 10). Spatial effectiveness of these maps is checked by receiver operating characteristics (ROC). The ROC curve is a useful method of representing the quality of deterministic and probabilistic detection and forecast systems (Swets 1988). The area under the ROC curve (AUC) characterizes the quality of a forecast system by describing the system's ability to anticipate correctly the occurrence or non-occurrence of pre-defined "events" (Yesilnacar and Topal 2005). The ROC curve plots the false positive rate on the X axis and 1—the false negative rate on the Y axis. It shows the trade-off between the two rates (Biggerstaff 2000). If the area under the ROC curve (AUC) is close to 1, the result of the test is excellent. On the contrary, the closer the AUC to 0.5, the fairer the result of the test is. The results of the ROC curve test are illustrated in Fig. 11. These curves indicate that the dataset 5 (Fig. 10e) has higher prediction performance than the other datasets. The area under the curve (AUC) for the dataset 5 is 0.84 which is an acceptable result for prediction purposes. In order to evaluate the sensitivities on the prediction capacities of different approaches, correct classification percentages (for the cut-off value of 0.5) and the root mean square error (RMSE) (Eq. 6) indices are also calculated.

$$\mathrm{RMSE} = \sqrt{\frac{1}{N}\sum_{i=1}^{N}(y - y')^2} \tag{6}$$

where N is the number of cases, y is the observed presence, and y' is the predicted presence. The predicted probability distributions for these sets are given in Fig. 12. Correct classification percentages and RMSE values of the datasets 1 and 2 are calculated as close to

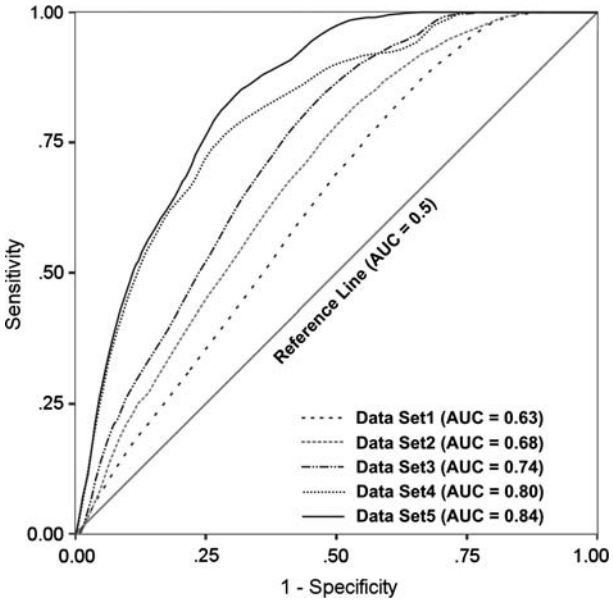


Fig. 11 Evaluation of receiver operating characteristics (ROC) curves relating to the different datasets within framework of backward stepwise logistic regression analyses

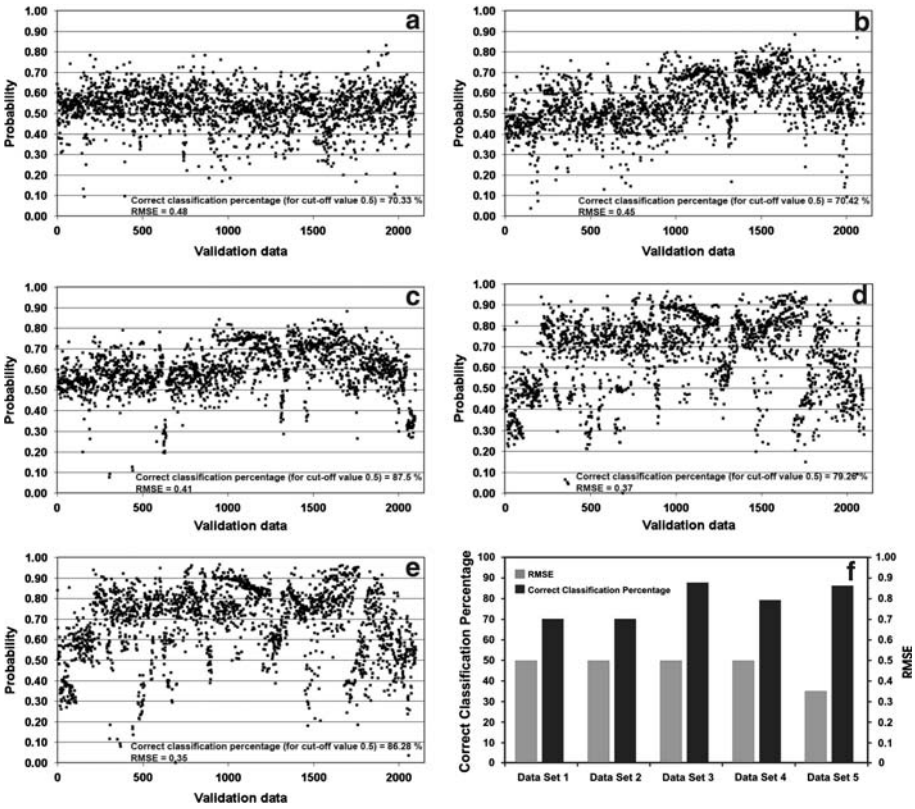


Fig. 12 Distributions of estimated probabilities of the validation datasets with correct classification percentages and RMSE indices with respect to different random samplings; (**a**) for dataset 1, (**b**) for dataset 2, (**c**) for dataset 3, (**d**) for dataset 4, (**e**) for dataset 5, and (**f**) Bar graphs of RMSE and correct classification percentage values

each other but the RMSE value of the dataset 2 is lower than that of dataset 1 (Fig. 10b). Therefore, this dataset is considered in order to analyses within datasets 3–5 (Fig. 10). Considering the correct classifications and the RMSE indices, the prediction capacity of the dataset 5 is significantly higher than that of the other datasets (Fig. 12f). Taking all of the analyses into consideration, it may be concluded that, the most appropriate landslide susceptibility map for the study area is obtained by using the dataset 5 (Fig. 10e) which has been obtained through the topographic parameters produced from the reconstructed DEM, lithological factors and geomorphologic units of this dataset are used together and 80% of presence (1) data is provided from the landslide inventory randomly for the training dataset.

In the study area, some of landslides, particularly scarp zones of those are located on the spatial domains having low susceptibility values (Fig. 10f). This is because these regions coincide with the boundary zones of the remnant plateau surfaces. The low beta coefficients of the morphological unit, remnant plateau surfaces cause the estimation of low susceptibility values. Considering the retrogressive character of the landsliding in the region, the continuum mass processes commonly occur throughout the boundary zones these remnant surfaces. Even though the low susceptibility values on these regions, this peculiarity might be concluded as evidence of a high consistency degree of the proposed

reconstruction methodology. Besides, the susceptibility values are commonly calculated as low on the accumulation zones of the mass movements (Fig. 10f). It is obviously an expected result because, as it is well known that the displacement of the natural material directly occurred on the depletion zone of a landslide event, not happened on the accumulation zone.

6 Results and conclusions

Although many publications on the landslide susceptibility mapping exist in the international literature, no studies considering the geomorphologic units before landsliding are encountered. Considering this lack, some comparisons between the landslide susceptibility maps produced by the actual and the reconstructed DEM, topographic parameters and the geomorphologic unit maps are made. The results and the conclusions obtained by the present study are summarized as follows:

(a) The landslides are one of the major earth surface processes. When geomorphologic unit maps including landslides are used in landslide susceptibility maps as a conditioning parameter, this results in conceptual conflict because the dependent variable is landslide. In order to avoid this problem, the geomorphologic units are not generally used in landslide susceptibility maps. However, if the reconstructed DEM reflecting the topographical conditions before landsliding is used, this problem will be eliminated. Moreover, one of the major aims of landslide susceptibility maps determines the zones having different landslide susceptibility values. For this reason, the topographic conditions at the time of failure provide considerable knowledge of the topographic conditions governing landslides. In the present study, these problems are put forward in detail.
(b) Employing the reconstruction method on the actual DEM, a possibility to use of geomorphologic units when preparing landslide susceptibility maps is provided. The geomorphologic units are probably the most important factors governing the landslide occurrence.
(c) Five landslide susceptibility maps of the study area are produced by using various parameter combinations. However, the susceptibility map produced by using the topographic parameters and geomorphologic units obtained from the reconstructed DEM exhibits the best results when considering not only statistical performance indices but also logical assessments.

As a further recommendation, reconstruction may better be considered when producing landslide susceptibility maps. The reconstruction will then provide an important contribution to the improvements of landslide susceptibility maps because the geomorphologic units can be implemented in landslide susceptibility maps without any conceptual contradiction. However, in order to apply the reconstruction method, dimensions of landslides have to be mapped. If such type and sized landslides do not exist, the reconstruction method cannot be applied. In this study, the reconstructed method is applied to the deep-seated landslides having a considerable areal extent. For this reason, the application of the reconstruction method to the other types of mass movements such as translational slides, flows, etc. is still open to improvement.

Acknowledgment We would like to extend our cordial thanks to S. Cigdem Erdogan (Head of Elective Foreign Languages Department) for her contribution to the improvement of the language of the paper.

References

AIGM (1995) Duzce Ili Dokuzdegirmen Koyu Jeolojik Etut Raporu. Afet Isleri Genel Mudurlugu (in Turkish, unpublished)

Atkinson PM, Massari R (1998) Generalized linear modeling of susceptibility to land sliding in the Central Apennines, Italy. Comput Geosci 24(4):373–385

Ayalew L, Yamagishi H (2005) The application of GIS-based logistic regression for landslide susceptibility mapping in the Kakuda–Yahiko Mountains, central Japan. Geomorphology 65:15–31

Barka AA (1992) The North Anatolian fault. Annales Tectonicae 6:174–195

Barka AA, Kadinsky-Cade K (1988) Strike-slip fault geometry in Turkey and its influence on earthquake activity. Tectonics 7:663–684

Biggerstaff BJ (2000) Comparing diagnostic tests: a simple graphic using likelihood ratios. Stat Med 19(5):649–663

Can T, Nefeslioglu HA, Gokceoglu C, Sonmez H, Duman TY (2005) Susceptibility assessments of shallow earthflows triggered by heavy rainfall at three sub catchments by logistic regression analyses. Geomorphology 72:250–271

Carrara A (1983) Multivariate models for landslide hazard evaluation. Math Geol 15(3):403–427

Childs C (2004) Interpolatin surfaces in ArcGIS spatial analyst. ArcUser July–September, 32–36. Internet version available at http://www.esri.com

Chung CJ, Fabbri A, Van Westen CJ (1995) Multivariate regression analysis for landslide hazard zonation. In: Carrara A, Guzetti F (eds) Geographical information systems in assessing natural hazards. Kluwer, pp 107–133

Chung CJ, Fabbri AG (1999) Probabilistic prediction models for landslide hazard mapping. Photogramm Eng Remote Sens 65(12):1389–1399

Clerici A, Perego S, Tellini C, Vescovi P (2002) A procedure for landslide susceptibility zonation by the conditional analysis method. Geomorphology 48:349–364

Clerici A, Perego S, Tellini C, Vescovi P (2006) A GIS-based automated procedure for landslide susceptibility mapping by the Conditional Analysis method: the Baganza valley case study (Italian Northern Apennines). Environ Geol 50(7):941–961

Cruden DM, Varnes DJ (1996) Landslide types and processes. In: Turner AK, Schuster RL (eds) Landslides: investigation and mitigation. National Academy Press, pp 36–75

Dietrich WE, Bellugi GD, Sklar LS, Stock JD (2003) Geomorphic transport laws for predicting landscape form and dynamics. In: Prediction in geomorphology geophysical monograph, vol 135, pp 1–30

Duman TY, Can T, Gokceoglu C, Nefeslioglu HA, Sonmez H (2006) Application of logistic regression for landslide susceptibility zoning of Cekmece Area, Istanbul, Turkey. Environ Geol 51:241–256

Emre O, Duman YT, Dogan A, Kecer M, Erkal T, Ozalp S, Yildirim N, Guner N (1999) Maden Tetkik Ve Arama Genel Mudurlugu 12 Kasım 1999 Duzce Depremi Saha Gozlemleri ve On Degerlendirme Raporu (16 Kasım 1999), MTA Raporu

Ercanoglu M, Gokceoglu C (2004) Use of fuzzy relations to produce landslide susceptibility map of a landslide prone area (West Black Sea Region, Turkey). Eng Geol 75(3/4):229–250

Gokasan E, Ustaomer T, Gazioglu C, Yasar YZ, Ozturk K, Tur H, Ecevitoglu B, Tok B (2003) Morphotectonic evolution of the Marmara Sea inferred from multi-beam bathymetric and seismic data. Geo-Mar Lett 23(1):19–33

Gokceoglu C, Aksoy H (1996) Landslide susceptibility mapping of the slopes in the residual soils of the Mengen region (Turkey) by deterministic stability analyses and image processing techniques. Eng Geol 44:147–161

Gokceoglu C, Sonmez H, Nefeslioglu HA, Duman TY, Can T (2005) The March 17, 2005 Kuzulu landslide (Sivas, Turkey) and landslide susceptibility map of its close vicinity. Eng Geol 81:65–83

Gorsevski PV, Gessler P, Foltz RB (2000) Spatial prediction of landslide hazard using logistic regression and Gz7. Conference on Integrating GIS and Environmental Modelling, Alberta, Canada, 9 pp

Guzzetti F, Carrara A, Cardinali M, Reichenbach P (1999) Landslide hazard evaluation: an aid to a sustainable development. Geomorphology 31:181–216

Guzzetti F, Reichenbach P, Cardinali M, Galli M, Ardizzone F (2005) Probabilistic landslide hazard assessment at the basin scale. Geomorphology 72(1–4):272–299

Guzzetti F, Reichenbach P, Ardizzone F, Cardinali M, Galli M (2006) Estimating the quality of landslide susceptibility models. Geomorphology 81(1–2):166–184

Ketin I (1948) Über die tektonisch-mechanischen Folgerungen aus den grossen Anatolischen Erdbeben des letzten Dezenniums. Geol Rundsch 36:77–83

Ketin I (1955) Akcakoca-Duzce bolgesinin jeolojik lovesi hakkinda memuar (1/100000 olcekli Eregli 22/3 ve Kismen Bolu 39/1 Paftalarinin Jeolojik Loveleri). MTA Enst Rap No: 2277

Lee S (2004) Application of likelihood ratio and logistic regression models to landslide susceptibility mapping using GIS. Environ Manage 34(2):223–232
Lee S (2005) Application of logistic regression model and its validation for landslide susceptibility mapping using GIS and remote sensing data. Int J Remote Sens 26(7):1477–1491
Lee S, Min K (2001) Statistical analysis of landslide susceptibility at Yongin, Korea. Environ Geol 40:1095–1113
Lee S, Pradhan B (2007) Landslide hazard mapping at Selangor, Malaysia using frequency ratio and logistic regression models. Landslides 4(1):33–41
Lee S, Ryu JH, Min K, Won JS (2003a) Landslide susceptibility analysis using GIS and artificial neural network. Earth Surf Process Landf 28:1361–1376
Lee S, Ryu JH, Lee MJ, Won JS (2003b) Use of an artificial neural network for analysis of the susceptibility to landslides at Boun, Korea. Environ Geol 44:820–833
Lee S, Ryu JH, Won JS, Park HJ (2004) Determination and application of the weights for landslide susceptibility mapping using an artificial neural network. Eng Geol 71:289–302
McCoy J, Johnston K (2001) Using ArcGIS spatial analyst. Esri Press New York, 280 pp
Menard S (1995) Applied logistic regression analysis. Sage University paper series on Quantitative applications in social sciences, vol 106, Thousand Oaks, California, 98 pp
Moore ID, Grayson RB, Ladson AR (1991) Digital terrain modeling: a review of hydrological, geomorphologic, and biological applications. Hydrol Process 5:3–30
Nefeslioglu HA, Duman TY, Durmaz S (2007) Landslide susceptibility mapping for a part of tectonic Kelkit Valley (Eastern Black Sea region of Turkey). Geomorphology 94:401–418
Ohlmacher CG, Davis CJ (2003) Using multiple regression and GIS technology to predict landslide hazard in northeast Kansas, USA. Eng Geol 69:331–343
Pekcan N (2000) Duzce-Akcakoca Bolgesinin Jeomorfolojisi. Filiz Kitabevi, Istanbul. 295 pp
Popescu ME (1990) A suggested method for reporting a landslide. UNESCO Working Party on World Landslide Inventory (WP/WLI). Bull Int Assoc Eng Geol 41:5–12
Remondo J, Gonzalez-Diez A, De Teran JRD, Cendrero A (2003) Landslide susceptibility models utilizing spatial data analysis techniques. A case study from the Lower Deba Valley, Guipuzcoa (Spain). Nat Hazards 30(3):267–279
Saroglu F, Emre O, Boray A (1987) Turkiye'nin diri faylari ve depremsellikleri. MTA Raporu, Rapor no: 8174, Ankara
Sengor AMC (1979) The North Anatolian transform fault: its age, offset and tectonic significance. J Geol Soc Lond 136:269–282
Suzen ML, Doyuran V (2004a) Data driven bivariate landslide susceptibility assessment using geographical information systems: a method and application to Asarsuyu catchments, Turkey. Eng Geol 71:303–321
Suzen ML, Doyuran V (2004b) A comparison of the GIS based landslide susceptibility assessment methods: multivariate versus bivariate. Environ Geol 45:665–679
Swets JA (1988) Measuring the accuracy of diagnostic systems. Science 240:1285–1293
Van Westen CJ, Rengers N, Soeters R (2003) Use of geomorphologic information in indirect landslide susceptibility assessment. Nat Hazards 30(3):399–419
Varnes DJ (1978) Landslides types and processes. In: Eckel EB (ed) In: Landslides and engineering practice. Highway Research Board Spec Rep 29:20–47
Wilson JP, Gallant JC (2000) Terrain analysis principles and applications. John Wiley & Sons Inc, Canada, 479 pp
Yesilnacar E, Topal T (2005) Landslide susceptibility mapping: a comparison of logistic regression and neural networks methods in a medium scale study, Hendek region (Turkey). Eng Geol 79:251–266
Zezere JL (2002) Landslide susceptibility assessment considering landslide typology. A case study in the area north of Lisbon (Portugal). Nat Hazards Earth Syst Sci 2:73–82